

Map-aided Navigation for Emergency Searches

Johan Wahlström, Pedro Porto Buarque de Gusmão, Andrew Markham, and Niki Trigoni
Department of Computer Science, University of Oxford, Oxford, UK
{johan.wahlstrom, pedro.gusmao, andrew.markham, niki.trigoni}@cs.ox.ac.uk

Abstract—Real-time positioning of emergency personnel has been an active research topic for many years. However, studies on how to improve navigation accuracy by using prior information on the idiosyncratic motion characteristics of firefighters are scarce. This paper presents an algorithm for generating pseudo observations of position and orientation based on standard search patterns used by firefighters. The iterative closest point algorithm is used to compare walking trajectories estimated from inertial odometry with search patterns generated from digital maps. The resulting fitting errors are then used to integrate the pseudo observations into a map-aided navigation filter. Specifically, we present a sequential Monte Carlo solution where the pattern comparison is used to both update particle weights and create new particle samples. Experimental results involving professional firefighters demonstrate that the proposed pseudo observations can achieve a stable localization error of about one meter, and offer increased robustness in the presence of map errors.

I. INTRODUCTION

Reliable indoor localization is a capability that would be of great help for firefighters in their mission to save lives and secure property [1]. However, emergency scenarios preclude the use of pre-deployed infrastructure and labor-intensive fingerprinting databases. Consequently, proposed navigation solutions have been based on odometry derived from body-worn cameras or inertial sensors. Unfortunately, stand-alone dead-reckoning systems will always be subject to position errors that accumulate with time. Moreover, dead-reckoning systems require knowledge of the initial navigation state. In the absence of measurements from positioning technologies, these problems can be mitigated by applying different types of navigation constraints. The two most common sources of navigation constraints are *map information* and *motion models*.

Map information is often fused with odometry by the use of particle filters. This means that the posterior density of the navigation state is represented by a weighted set of samples (particles). When a particle collides with a wall, it is either eliminated or has its weight reduced. In this way, the navigation estimates are continuously adjusted based on the floor plan [2]. The incorporation of accurate map information will typically yield a significant performance improvement. However, in emergency scenarios, floor plans are often outdated. Hence, one of the key challenges of firefighter positioning is the design of algorithms that are robust to map errors.

An example of a motion model is the zero-velocity update (ZUPT) that is used in foot-mounted inertial navigation systems (INSs) [3]–[5]. A ZUPT-aided INS uses a zero-velocity detector to determine when the foot is approximately stationary. When this is the case, the navigation system performs a measurement update based on pseudo observations of zero

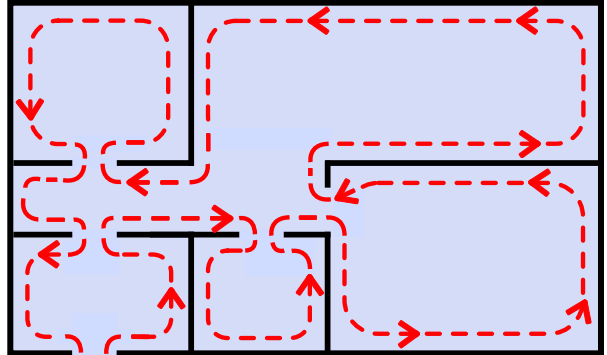


Fig. 1. Firefighters often search a building by walking along the wall in what is known as a directional search. The arrows indicate the direction of a right-hand directional search. A left-hand search is obtained by traversing the trajectory in the opposite direction.

velocity. Conducted experiments indicate that this constraint is still useful in firefighter positioning. However, this is only the tip of the iceberg; there is much more information hidden in the standardized motion patterns of firefighters (see Fig. 1), which so far has been overlooked. The literature contains little information on how to transform knowledge about firefighting procedures into useful motion models.

This paper presents the first method for firefighter localization that fuses inertial odometry and map information with a motion model describing firefighters' tendency to follow left- or right-hand search patterns. Our contributions are as follows:

- We propose the idea of using standardized search patterns within firefighting to improve localization accuracy.
- We explain how to generate such patterns from a digital map, and how to compare the generated search patterns with position trajectories derived from odometry.
- We tackle the challenging cases of i) unknown initial position and ii) map errors, and demonstrate the benefits of the proposed navigation system in these scenarios.
- We evaluate the proposed approach with data from simulated emergency scenarios in two different buildings.

In principle, the proposed navigation system can be used with any odometry system (e.g., camera, inertial, mmWave radar, etc.). This paper uses inertial odometry, which is attractive due to the low cost of inertial sensors, and their robustness to adverse environment conditions such as heavy smoke. The pattern comparison is particularly useful when the uncertainty of the navigation state is large. Therefore, it is ideal for the unprepared emergency scenario where map errors may cause the navigation system to repeatedly lose track of the true

navigation state.

The remainder of the paper is organized as follows: Section II provides the necessary background on firefighter movements in emergency scenarios, while Section III provides an overview of the system architecture. Section IV provides a detailed description of the different system components. Further, Section V analyses the performance of the proposed and competing approaches in two distinct settings. The paper is concluded in Section VI.

II. FIREFIGHTER MOVEMENTS IN EMERGENCY SCENARIOS

The motion characteristics of firefighters in emergency scenarios are in many ways different from those of civilians during normal day-to-day walking [6]–[9]. Firefighters may for example sweep the area around them with their hands and feet to increase visibility and detect loose cables, casualties, or other unseen objects; get down on their knees for protection against flashovers and backdrafts before opening doors; and walk backwards down through stairs or when carrying casualties. Searches tend to fall in two categories. A *primary search* is performed when living victims may still be inside the building, and must therefore be conducted as quickly as conditions warrant (the walking speed still tends to be slow in comparison to the typical human walking speed). The search is generally conducted in a harsh environment with intense heat and poor visibility. Subsequently, a more thorough *secondary search* is performed to ensure that no one is left in the building. At this point, the fire is usually under control or fully extinguished [10]. Next, we discuss standardized search procedures for primary searches, where the need for localization solutions is the greatest.

Searches are conducted in teams of two to four (typically two) firefighters who maintain physical contact during the search. By following established search patterns, a team of firefighters can quickly and thoroughly search a building, with low risk of disorientation. In residential and small commercial buildings, firefighters often perform a *directional search*. Directional searches follow either a left- or a right-hand search pattern. During a right-hand search, the firefighter turns right at each entry point, and turns left in each corner. Analogous statements can be made regarding left-hand searches. The team will normally walk around large items of furniture, such as beds or tables, while carefully searching them. Directional left- and right-hand search patterns are illustrated in Fig. 1.

In complex multi-compartment structures (rooms “behind” rooms), the directional search may be replaced by the *compartmental search* which provides a methodological approach for mapping out compartments. In a compartmental search, the team first searches the room or compartment they are currently in using a left- or right-hand search pattern. During the search, the firefighters make sure to identify all of the doors in the compartment (excluding the one from which they entered the compartment), without immediately searching the rooms that they lead to. After completing a full left- or right-hand search of a compartment, they walk back the same way to the first identified door. The procedure is then iterated, starting

in the compartment behind this door. One problem with both directional and compartmental searches is that inner walls not connected to the outer walls will not be searched when adhering to standard search patterns. Assuming that such inner walls are detected, this problem can be tackled by performing a separate, targeted search around these inner walls.

The choice of whether to perform a directional or a compartmental search is made by the incident commander and is then communicated using voice radio to all firefighters. According to informal estimates from firefighters at Hampshire Fire and Rescue Service, UK, their team start off with a directional search in more than 90% of their searches. Accordingly, this paper focuses on motion models based on directional search patterns. However, the general idea can equally well be applied to compartmental searches after a small adjustment of the pattern extraction algorithm. Most of the information in this section has been gathered from firefighters at Hampshire Fire and Rescue Service, UK. Although the routines of other fire departments may differ, directional searches are widely used by firefighters all over the world.

III. ESTIMATION ARCHITECTURE

The high-level information flow of the proposed navigation system is shown in Fig. 2. The blue boxes in the figure describe components in standard map-aided odometry. To begin with, sensor measurements are collected from foot-mounted inertial sensors (see the top left of Fig. 2). These measurements are used to estimate the displacement in between sampling instances. Position estimates are then computed by recursively integrating the estimated displacements. To prevent the sensor errors from causing the position error to grow without bound, a digital map is generated from an available floor plan (see the bottom left of Fig. 2). Finally, the information from the odometry and the map is fused to produce the final navigation solution (see the right part of Fig. 2).

The white boxes in Fig. 2 give a conceptual description of the proposed method for generating and utilizing pseudo observations of position and orientation. The digital map is used to extract sequences of positions typically present in directional searches. Similar segments can be obtained by integrating the displacement estimates produced by the odometry over a given time period, just as one would during dead-reckoning. Each trajectory generated from the odometry is then compared to trajectories generated from the digital map. The similarity between a pair of trajectories acquired from the two sources is used to weight the pseudo observations. Specifically, if a search pattern generated by the odometry is very similar to a search pattern generated from the map, the positions in the latter search pattern can be used to construct an observation that is assigned a high likelihood. In the last step, the observations generated from the pattern comparison are fused with information from the odometry and the map to increase the update rate and enhance the performance of the navigation solution (see the right part of Fig. 2).

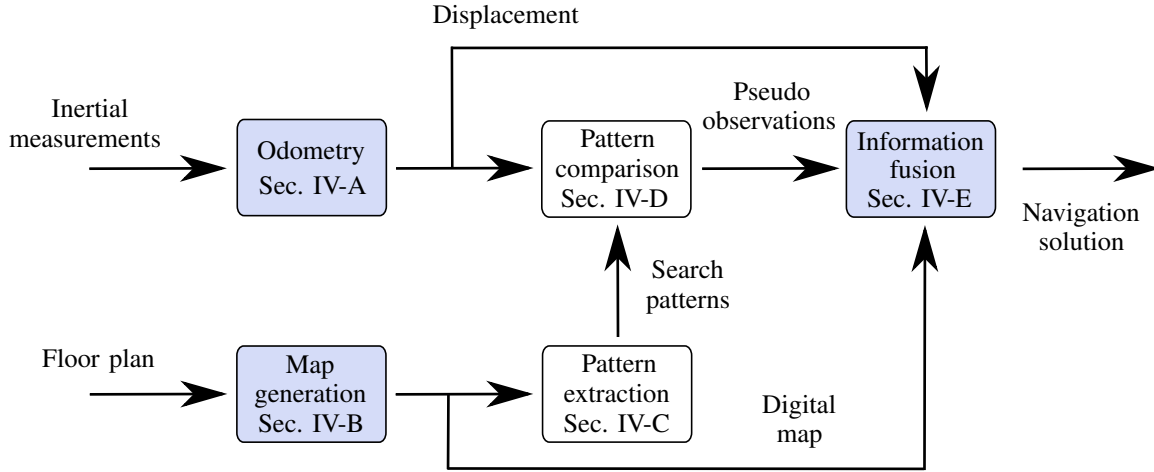


Fig. 2. Process diagram illustrating the information flow within the proposed navigation system. The boxes “Odometry”, “Map generation”, and “Information fusion” describe components in standard map-aided navigation based on odometry, while the boxes “Pattern comparison” and “Pattern extraction” make up the novel method for generating pseudo observations based on common search routines within firefighting.

IV. COMPONENTS IN NAVIGATION SYSTEM

This section describes our implementation of the different subcomponents illustrated in Fig. 2.

A. Odometry

The odometry is based on measurements collected from foot-mounted, six degrees of freedom inertial measurement units. By integrating the measurements in a ZUPT-aided INS [11], we obtain three-dimensional estimates of position, velocity, and orientation with the same update rate as the measurements. These estimates are then fed to the pattern comparison algorithm and to the information fusion filter.

B. Map Generation

A digital map is constructed by letting each wall in a floor plan¹ be represented by an edge in a topological graph. Thus, each node is associated with a two-dimensional position, representing the start or end point of a wall. The constructed map makes no distinction between doors and openings of the same size. Multi-floor maps can be created using a set of topological graphs, each representing the walls of a stairway or a specific floor.

C. Pattern Extraction

This subsection describes how to extract search patterns from a map. To begin with, a two-dimensional orthogonal grid of square cells with a pre-defined grid spacing is distributed over the map area. A sequence of nodes representing a directional search may then be constructed in the following way: The node that is closest to the entry of the building is chosen as the first node. The second node is chosen so that it is adjacent to the first node (i.e., the distance between the first two nodes is equal to the grid spacing), and so that it

is the next node that is reached by following a right-hand search along the grid. Similarly, the n th node is chosen as the node that is reached by continuing a right-hand search from the $(n-1)$ -th node. This continues until the sequence returns to the first node. The process results in a position sequence $\{\mathbf{p}_n\}_{n=1}^N$, consisting of N nodes. Here, \mathbf{p}_n denotes a two-dimensional position. The node \mathbf{p}_N is assumed to be adjacent to \mathbf{p}_1 . An example of a generated node sequence is given by the blue circles in Fig. 3.

The search patterns used for the pattern comparison are constructed as overlapping subsets (of fixed length) of the node sequence. Two overlapping search patterns are illustrated with black lines drawn around the nodes in the bottom right of Fig. 3, and separately in Fig. 4. If there are inner walls that are not connected to the outer walls (see the top right of Fig. 3), one may have to create additional node sequences where the first node is chosen among nodes close to these inner walls. A node sequence resulting from such a process is illustrated using grey circles in Fig. 3. All in all, the pattern extraction results in M node sequences $\{\{\mathbf{p}_n^{(m)}\}_{n=1}^{N_m}\}_{m=1}^M$. Here, $\mathbf{p}_n^{(m)}$ denotes the n th two-dimensional position in sequence m , and N_m is the number of nodes in the m th sequence. For floors that are not based on rectangular shapes other methods for extracting search patterns would have to be considered. One approach could for example be to construct search patterns from lines drawn along, but just inside, the walls. As an example, a wall in the shape of an arc would then result in a search pattern also in the shape of an arc but with a different radius.

D. Pattern Comparison

In what follows, we describe how the iterative closest point (ICP) algorithm² is used to compare position trajectories constructed from the odometry (see Section IV-A) with the

¹Today, many fire departments have access to floor plans from a large number of commercial and public buildings. The availability of floor plans is expected to increase in the future.

²ICP is a commonly used algorithm for finding the optimal (in terms of least squares) rotational and translational transformation between two multidimensional sets of points [12].

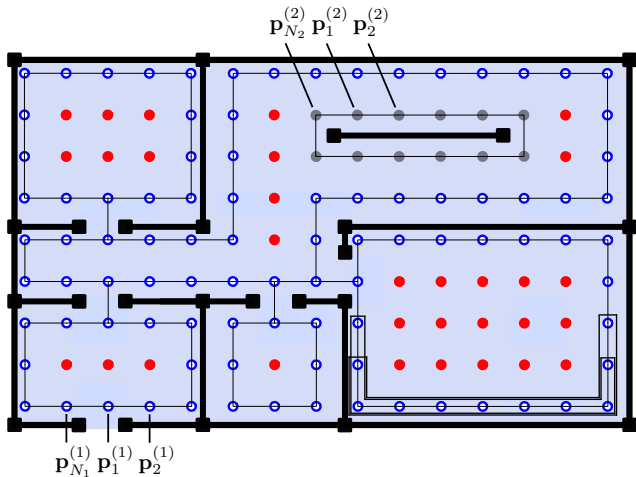


Fig. 3. Illustration of map generation and pattern extraction. The nodes and edges in the map are represented by solid black squares and black lines, respectively. The blue and grey circles represent two separate node sequences.

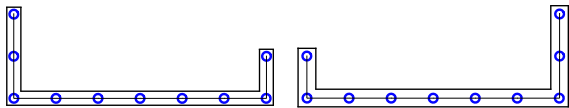


Fig. 4. Two search patterns extracted from the bottom right of Fig. 3.

search patterns generated from the map (see Section IV-C). Specifically, consider a trajectory $\{\mathbf{x}_\ell\}_{\ell=\ell_1}^k$ generated from the odometry. Here, \mathbf{x}_ℓ denotes a two-dimensional position in the horizontal plane, k is the sampling instance of the latest inertial measurements, and ℓ_1 is chosen so that the trajectory is of length d . Now, the task at hand is to assess how well the search patterns, generated from the digital map, matches the considered trajectory. This is done in two steps.

1) *Rotation of odometry trajectory*: First, note that most buildings, rooms, and corridors are constructed with a rectangular layout. As a result, most pedestrian walking can be expected to be in one of four principal headings. This is especially true for firefighters who walk along walls. Therefore, the trajectory $\{\mathbf{x}_\ell\}_{\ell=\ell_1}^k$ is first rotated so that it aligns with the four principal headings of the building. Specifically, the trajectory is rotated so as to minimize the average distance between the displacement vector angle and the closest horizontal or vertical direction. In mathematical terms, we apply a rotation of angle

$$\hat{\phi} = \arg \min_{\phi} C(\phi) \quad (1)$$

to the trajectory in the horizontal plane. Here, we have defined $C(\phi) \triangleq \sum_{\ell=\ell_1}^{k-1} \min(|\theta_\ell + \phi - \pi|, |\theta_\ell + \phi - \pi/2|, |\theta_\ell + \phi|, |\theta_\ell + \phi + \pi/2|)$ where θ_ℓ is the direction (angle) in the horizontal plane of the displacement vector $\mathbf{x}_{\ell+1} - \mathbf{x}_\ell$.

Although ICP does consider rotational transformations to align the two trajectories, the final result will be dependent on the relative orientation of the trajectories fed to the ICP algorithm. Thus, each comparison between the odometry trajectory and a search pattern is investigated with four different initializations. These four initializations correspond to rotating

the odometry to the four principal directions³, i.e., applying an additional rotation with an angle of $0, \pi/2, \pi, \text{ or } 3\pi/2$.

2) *The iterative closest point algorithm*: The ICP algorithm is now used to compare the rotated trajectories with the search patterns generated from the digital map. The comparison between the odometry trajectory and the search patterns constructed from the m th position sequence $\{\mathbf{p}_n^{(m)}\}_{n=1}^{N_m}$ is summarized using a matrix \mathbf{E}_m of ICP root-mean-square errors (RMSEs) with dimension $N_m \times 2$. Here, the first dimension signifies different possible starting nodes η in the search pattern $\{\mathbf{p}_n^{(m)}\}_{n=\eta}^{\eta+\Delta N}$ (ΔN is chosen so that the length of $\{\mathbf{p}_n^{(m)}\}_{n=\eta}^{\eta+\Delta N}$ is as close as possible to the length of the odometry trajectory). The second dimension of \mathbf{E}_m corresponds to the alternatives of using either the first position $\mathbf{p}_\eta^{(m)}$ (corresponding to a left-hand search) or the last position $\mathbf{p}_{\eta+\Delta N}^{(m)}$ (corresponding to a right-hand search) in the search pattern as a position measurement. This decision is made based on whether the last position in the odometry trajectory, rotated and translated using the output from the ICP algorithm, is closest to $\mathbf{p}_\eta^{(m)}$ or $\mathbf{p}_{\eta+\Delta N}^{(m)}$. Since we consider four possible rotations of the odometry trajectory, \mathbf{E}_m stores the minimum RMSE obtained from the corresponding four ICP algorithms. The matrix \mathbf{E}_m is moreover associated with the two tensors \mathbf{Pos}_m and \mathbf{Hea}_m of sizes $N_m \times 2 \times 2$ and $N_m \times 2$, respectively. The former specifies position observations and the latter specifies heading observations.

In summary, the trajectory $\{\mathbf{x}_\ell\}_{\ell=\ell_1}^k$, estimated using foot-mounted inertial measurements, is compared to search patterns emulating a directional search based on a digital map. For every position sequence $\{\mathbf{p}_n^{(m)}\}_{n=1}^{N_m}$ extracted from the map, the pattern comparison produces

- \mathbf{E}_m – A matrix of RMSEs from the ICP algorithm.
- \mathbf{Pos}_m – A tensor of position observations.
- \mathbf{Hea}_m – A matrix of heading observations.

The pattern comparison is summarized in Algorithm 1.

E. Information Fusion

This subsection describes how the position and heading observations from the pattern comparison (see Section IV-D) are fused together with the odometry (see Section IV-A) and the map information (see Section IV-B). For this we use a particle filter where each particle is associated with a two-dimensional position estimate and a heading estimate. The filter includes time updates as well as measurement updates based on the pattern comparison and the map information. The time update consists of two steps. In the first step, the particle estimates are updated based on the odometry since the last update. In the second step, random noise is added individually to all particles estimates.

Map information is incorporated by eliminating any particle whose position estimate crosses a wall. For the pseudo obser-

³In scenarios where magnetic disturbances are negligible, magnetometers may be used to get estimates of the firefighter's walking direction. In this case, the relative orientation of the odometry trajectory and the map will be known and the ICP algorithm does not need to be run with multiple initializations.

Algorithm 1 : Pattern comparison.

- 1: Rotate the search pattern from the odometry with the angle $\hat{\phi}$ from (1).
- 2: for $m = 1, \dots, M$ (for every node sequence)
- 3: for $\eta = 1, \dots, N_m$ (for every start node)
- 4: for $i = 1 : 4$ (for the four principal directions)
- 5: *Rotate odometry search pattern*: Rotate the odometry search pattern in the horizontal plane with the angle $\theta^{(i)}$, where $\theta^{(1)} = 0$, $\theta^{(2)} = \pi/2$, $\theta^{(3)} = \pi$, and $\theta^{(4)} = 3\pi/2$.
- 6: *Iterative closest point*: Apply the ICP algorithm to find 1) the ICP RMSE ξ ; 2) the optimal ICP rotation $\hat{\mathbf{R}}$ and translation $\hat{\mathbf{t}}$ that transform positions in the odometry search pattern to positions in the map search pattern.
- 7: *Rotate and translate odometry trajectory based on ICP*: Transform the last position in the odometry search pattern to the map search pattern using $\hat{\mathbf{R}}$ and translation $\hat{\mathbf{t}}$. The result is denoted $\mathbf{x}_k^{\text{transf}}$.
- 8: if $\|\mathbf{x}_k^{\text{transf}} - \mathbf{p}_\eta^{(m)}\| < \|\mathbf{x}_k^{\text{transf}} - \mathbf{p}_{\eta+\Delta N}^{(m)}\|$
- 9: $\mathbf{e}(i, 1) = \xi$, $\mathbf{e}(i, 2) = \infty$
- 10: else
- 11: $\mathbf{e}(i, 1) = \infty$, $\mathbf{e}(i, 2) = \xi$
- 12: end
- 13: end
- 14: *Store ICP errors, position observations, and heading observations*:

$$\mathbf{E}_m(\eta, 1) = \min_i \mathbf{e}(i, 1)$$

$$\mathbf{E}_m(\eta, 2) = \min_i \mathbf{e}(i, 2)$$

$$\mathbf{Pos}_m(\eta, 1, :) = \mathbf{p}_\eta^{(m)}$$

$$\mathbf{Pos}_m(\eta, 2, :) = \mathbf{p}_{\eta+\Delta N}^{(m)}$$

$$\mathbf{Hea}_m(\eta, 1) = \arctan2(-[\Delta \mathbf{p}_\eta^{(m)}]_2, -[\Delta \mathbf{p}_\eta^{(m)}]_1)$$

$$\mathbf{Hea}_m(\eta, 2) = \arctan2([\Delta \mathbf{p}_{\eta+\Delta N}^{(m)}]_2, [\Delta \mathbf{p}_{\eta+\Delta N}^{(m)}]_1)$$

where $\Delta \mathbf{p}_n^{(m)} \triangleq \mathbf{p}_{n+1}^{(m)} - \mathbf{p}_n^{(m)}$ and $\mathbf{A}(n, n')$ denotes the (n, n') th element of matrix \mathbf{A} .

15: end

16: end

variations from the pattern comparison, we use the exponential likelihood function

$$p_{\text{likelihood}}^{(i)} = \exp(-E^{(i)}/\sigma^2) \quad (2)$$

where σ is a design parameter and $E^{(i)}$ is the RMSE of the observation whose associated navigation state most closely resembles that of particle i . Specifically, for each particle i , one first finds the two identical positions in \mathbf{Pos}_m that are closest to the position of particle i . One then chooses the position

whose associated heading estimate⁴ is closest to the heading estimate of particle i . The associated RMSE in \mathbf{E}_m is used in (2). Finally, the weight $w_k^{(i)}$ of particle i at sampling instance k is updated according to

$$w_{k+1}^{(i)} = \frac{p_{\text{likelihood}}^{(i)} \cdot w_k^{(i)}}{\sum_{i=1}^{N_p} p_{\text{likelihood}}^{(i)} \cdot w_k^{(i)}} \quad (3)$$

where N_p denotes the number of particles. All particles that cross a wall or have a weight below some design parameter ϵ are replaced at random by identical copies of the remaining particles.

One of the main challenges of conventional map-aided inertial odometry is the initialization of the navigation estimate [13]. We mitigate this problem by sampling new particles from the generated pseudo observations. Hence, after each measurement update based on the pattern comparison the q percent particles with the lowest weight are replaced by particles whose navigation states are taken at random (in proportion to the likelihood function $p_{\text{likelihood}}^{(i)}$) from the navigation states in \mathbf{Pos}_m and \mathbf{Hea}_m . To increase the particle diversity, noise was added to the navigation states of all particles that were resampled in this way. In the experimental section, we investigate the performance of the navigation system both with and without this type of resampling.

V. EXPERIMENTS

A performance evaluation was conducted using data collected with both a professional firefighter and a civilian. This section describes in turn the studied data sets, the parameter selection, the performance of the navigation system that was characterized in Sections III and IV, and how the navigation system may be used for the detection of map errors.

A. Data

Data was recorded in two buildings. The first data set consists of 73 minutes of data representing 16 separate searches (nine of which were left-hand searches) conducted by a firefighter performing directional searches and attempting to replicate normal firefighter movements during emergency searches. The second data set consists of 20 minutes of data from two left-hand searches performed by a civilian imitating firefighter movements. All data was recorded at 100 [Hz] from a foot-mounted Xsens MTi-3-8A7G6-DK IMU. The IMU was placed on the foot closest to the wall, i.e., the foot that was not used for sweeping. In the first data set, the firefighter moved in an area of size 70 [m²] where a VICON system with 17 infrared cameras recorded ground truth position data at 100 [Hz]. To make the positioning problem more challenging, the navigation system was run in a larger area of size 125 [m²].

⁴Note that the heading observations in \mathbf{Hea}_m represent the walking direction of the firefighter whereas the yaw estimates produced by the odometry is the yaw estimate of the inertial measurement unit. Hence, at each measurement update the relative orientation between the inertial measurement unit and the walking direction is estimated [2]. The yaw estimates are then transformed to walking direction estimates before being compared with the observations in \mathbf{Hea}_m .

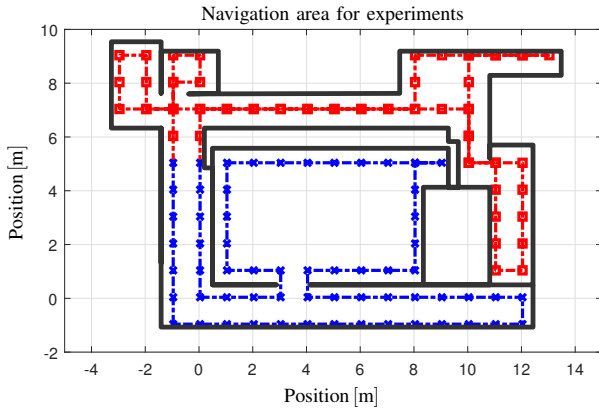


Fig. 5. Area where the first data set was collected. The search pattern generated from the map is illustrated with blue crosses (in the area where the VICON system was installed and the firefighter performed searches) and red squares (in the remaining area).

The second data set was recorded in a separate building in an area of size $253 \text{ [m}^2\text{]}$. Since there was no positioning system available for recording ground truth in this environment, artificial ground truth data was created manually based on the recorded odometries, the available map, and knowledge of the true trajectory. This resulted in ground truth position data at ten uniformly spaced points in time (for each of the two data recordings). The two considered navigation areas are illustrated in Figs. 5 and 6. Due to limitations in the spatial coverage of the VICON system and in the accessibility of certain rooms, the participants in the experiments were instructed to treat some doors or openings as walls. To make the scenario as realistic as possible, these doors and openings were treated as walls also in the map used for navigation.

B. Parameter Selection

Since the walking speed was rather low, the odometry was downsampled to 2 [Hz] before it was used in the pattern comparison and in the particle filter. Further, the grid spacing was set to 1 [m] (this is sufficiently small to obtain nodes in fairly narrow hallways, etc.), the pattern comparison used search patterns of length $d = 20 \text{ [m]}$, and a new pattern comparison was performed when the firefighter had walked 2 [m] since the last one. In the time update of the particle filter, Gaussian noise with a standard deviation of 0.12 [m] (along each spatial direction) and $2 \text{ [}^\circ\text{]}$ per traversed meter was added to the position and yaw estimates, respectively. These two parameters were set by a quick visual inspection of how the particle distribution spread out over time in the navigation area. Similarly, we used $\sigma = 0.1 \text{ [}\sqrt{\text{m}}\text{]}$ in the likelihood function (2). Further, the particle weight floor and the percentage of resampled particles from the pseudo observations were set to $\epsilon = 0.01 \cdot 1/N_p$ and $q = 10 \text{ [%]}$, respectively. Gaussian noise with a standard deviation of 0.5 [m] (along each spatial direction) and $25 \text{ [}^\circ\text{]}$ was added to the reinitialized position and yaw estimates, respectively. The filter was run with $N_p = 500$ particles and the RMSEs were computed from the minimum

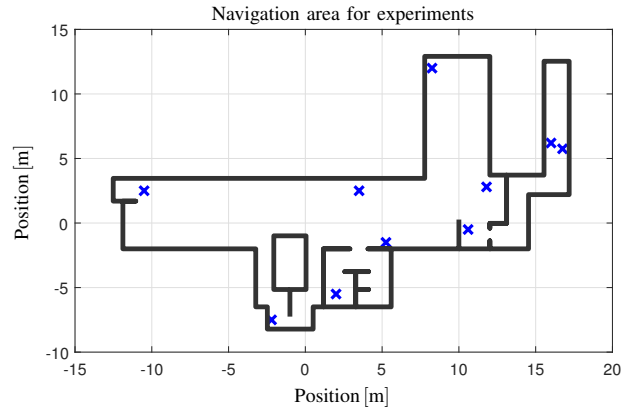


Fig. 6. Area where the second data set was collected. The positions of the evaluation points are marked with blue crosses.

mean square error estimate (the weighted mean of the particle distribution) as averaged over 10 runs.

C. Performance of Navigation System – Data Set 1

Fig. 8 illustrates the RMSE for the horizontal position estimates on the first data set. The figure shows the results for the navigation system with and without pseudo observations, as well as with and without prior information on the initial navigation state (in the latter case, the particles were initialized at random over the navigation area). Further, the figure displays the performance with and without the resampling step described in the last paragraph of Section IV-E. As seen from Fig. 8 (a), the pseudo observations from the pattern comparison does not improve the performance of the localization system when the initial navigation state is known. Both with and without pseudo observations, the navigation system maintains a RMSE around or below one meter for five minutes; no obvious overall difference in performance can be seen. However, a different picture is painted by Fig. 8 (b), which considers the more realistic case where there is no information on the initial navigation state. In this case, the conventional particle filter will in many runs not be able to find the true navigation solution, and the average RMSE is around four meters. On the other hand, when using the proposed pseudo observations together with the resampling step the filter stabilizes at a RMSE of about one meter after about two and a half minutes (note that the pattern comparison cannot be performed without a decent amount of odometry). Since it often takes a firefighter half an hour or more to search a building, a “settling time” in this order of magnitude means that the navigation system will provide the firefighter with a reliable localization solution most of the time that they spend inside the building.

D. Performance of Navigation System – Data Set 2

Fig. 7 displays the performance averaged over the two searches in the second data set. The resampling step can be seen to have a significant negative impact on the localization accuracy both without and without knowledge of the initial

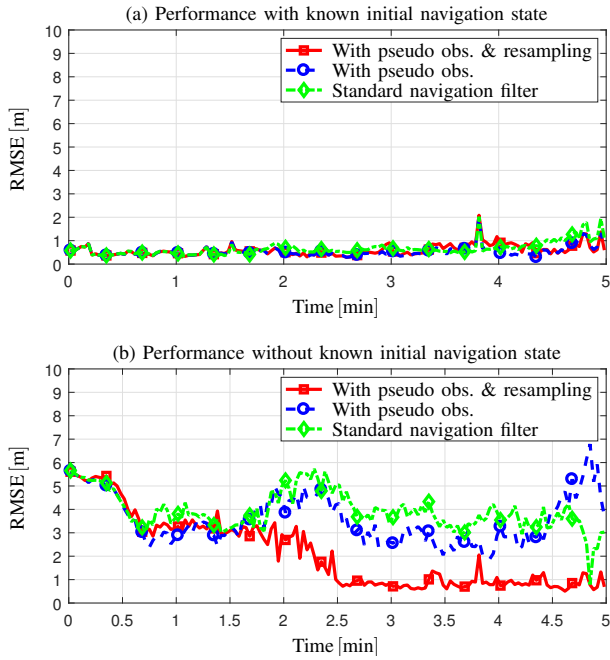


Fig. 7. Performance of the proposed navigation system on the first data set. The two figures (a) and (b) display the horizontal position error with and without prior information on the initial navigation state.

navigation state. However, Fig. 7 (b) shows that without knowledge of the initial navigation state, the best localization accuracy is achieved by using the pseudo observations to update the particle weights, but not to resample new particles. In conclusion, Sections V-C and V-D demonstrate that the proposed navigation system have the potential to yield a significant increase in localization accuracy in emergency scenarios. However, the inclusion of a resampling step where new particles are generated based on the created pseudo observations can have both a positive and a negative impact on the navigation accuracy. One possible explanation to the observed discrepancies in this matter lies in the size of the navigation area. Since the navigation area in Fig. 6 is approximately twice as large the navigation area in Fig. 5, there will be much more search patterns generated from the map of the former area. Hence, the risk of poor pattern matching is also larger in this case, and the resampling step may therefore cause the navigation system to be thrown off course.

E. Detection and Characterization of Map Errors

In many situations, the available floor plan will either contain errors or ambiguous features, or not be sufficiently updated. If the floor plan is for example missing a door, this may cause the particle filter to degenerate. Next, we will demonstrate how the proposed navigation system can be used to both detect map errors, and rapidly find the correct navigation state if map errors cause the particles to disintegrate. For this purpose, we considered one of the search patterns from the first data set, and simulated a map error by changing the position of a door in the map. Fig. 9 (a) shows the variance (summed over both horizontal directions) of the

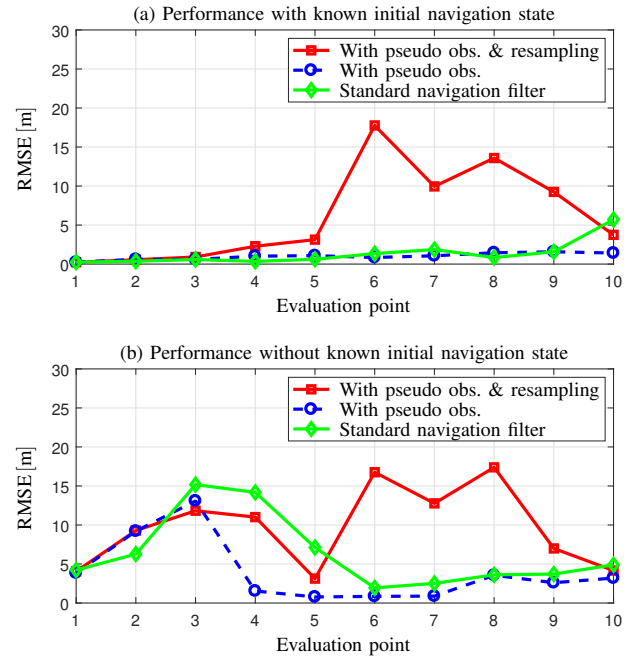


Fig. 8. Performance of the proposed navigation system on the second data set. The two figures (a) and (b) display the horizontal position error with and without prior information on the initial navigation state.

position estimates as estimated from the particle filter versus the corresponding squared position error. The search has been divided into four periods based on whether the estimated variance exceeds or falls below $3 \text{ [m}^2\text{]}$. The first period is before the filter has converged; in the second period, the filter converges and reaches a position error around or below 1 [m] ; in the third period, the uncertainty increases due to the map error; and in the fourth period, the filter converges again. Fig. 9 displays the position estimates produced by the proposed navigation system in periods 2 and 4. In addition, the figure shows the position smoothing estimates obtained by using only the odometry from the inertial sensors during period 3, and the starting and ending points obtained from the navigation states at the end of period 2 and at the start of period 4, respectively. During period 3, the odometry estimates cross the wall at a position that is much closer to the true door (see Fig. 5) than the door displayed in Fig. 9 (b). In summary, the results shown in Fig. 9 demonstrate the following: sudden increases in the estimated position variance can be used to indicate that the filter may have been disturbed by map errors. Incident commanders and firefighters can then put larger trust in the position estimates that are produced when the estimated position variance is small. Moreover, they can, based on the position estimates, the map, and possibly also inertial odometry in the periods where the position variance estimated using the particle filter is large, obtain some clues on the extent and character of possible map errors.

VI. CONCLUDING REMARKS

As part of their job, firefighters are expected to perform life-saving missions in dangerous environments with poor

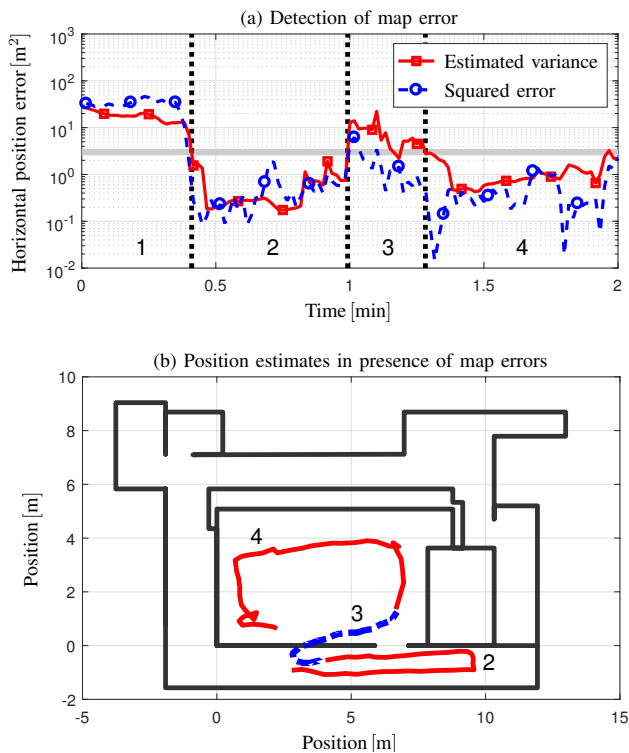


Fig. 9. Illustration of how the proposed navigation system could be used to detect and mitigate map errors. Figure (a) shows the variance (summed over both horizontal directions) of the position estimates as computed from the particle filter versus the corresponding squared position error for a given search. Figure (b) displays the navigation solution computed using the proposed navigation system during periods 2 and 4 and the odometry computed using the inertial sensors over period 3.

visibility. If accurate firefighter localization was available as a seamless and robust on-demand service, this would greatly facilitate the planning and coordination of the deployed units, and thereby increase the chance of a successful operation. Although there exists a considerable amount of research on indoor positioning motivated by firefighting scenarios, most studies have ignored the fact that firefighters do not move at random inside a building. On the contrary, firefighters will often follow well-rehearsed search procedures that in detail dictate how they will move. Since the search procedures do not simply specify a location or a direction that the firefighter is expected to follow, standard map-matching techniques do not suffice, and there is a need for more sophisticated methods that can handle intricate search patterns generated from existing map information.

This paper has presented a navigation system that utilizes prior information on the motion characteristics of firefighter searches to improve the navigation performance. Search patterns representing directional searches were first generated from a map of the building. The search patterns were then compared to position trajectories generated from foot-mounted inertial sensors using the iterative closest point algorithm. The comparison was used to generate pseudo observations of position and orientation which were fused together with

inertial odometry and map information to produce the final navigation solution.

Without knowledge of the initial navigation state, the navigation system with pseudo observations reached a steady-state RMSE of about one meter on data collected with firefighters. The proposed navigation system thereby outperformed the corresponding conventional navigation system by a great margin. Further, the performance evaluation indicated that the information provided by the pattern comparison is of most use before the navigation filter has converged to the true navigation state. As demonstrated in a separate example, this also implies that the filter is particularly useful when the estimation uncertainty has increased due to for example map errors. Additional experiments conducted with civilians in a larger navigation area indicated that the optimal implementation differs depending on the considered navigation area. This motivates further studies into how information from directional searches can be utilized in large navigation areas and in the presence of heavy furniture, map errors, and deviations from standardized search procedures.

REFERENCES

- [1] A. F. G. Ferreira, D. M. A. Fernandes, A. P. Catarino, and J. L. Monteiro, "Localization and positioning systems for emergency responders: A survey," *IEEE Commun. Surveys Tuts.*, vol. 19, no. 4, pp. 2836–2870, 2017.
- [2] P. Davidson and R. Piché, "A survey of selected indoor positioning methods for smartphones," *IEEE Commun. Surveys Tuts.*, vol. 19, no. 2, pp. 1347–1370, 2017.
- [3] I. Skog, P. Händel, J. O. Nilsson, and J. Rantakokko, "Zero-velocity detection — An algorithm evaluation," *IEEE Trans. Biomed. Eng.*, vol. 57, no. 11, pp. 2657–2666, Nov. 2010.
- [4] J. Wahlström, I. Skog, and P. Händel, "Inertial sensor array processing with motion models," in *IEEE Int. Conf. Inf. Fusion*, Cambridge, UK, Jul. 2018, pp. 788–793.
- [5] J. Wahlström, I. Skog, F. Gustafsson, A. Markham, and N. Trigoni, "Zero-velocity detection — A Bayesian approach to adaptive thresholding," *arXiv e-prints*, p. arXiv:1903.07929, Mar. 2019.
- [6] L. Yang and T. Zhao, "Data mining and ergonomic evaluation of firefighter's motion based on decision tree classification model," in *Advanced Research on Computer Sci. and Inf. Eng.*, G. Shen and X. Huang, Eds. Springer Berlin Heidelberg, 2011, pp. 212–217.
- [7] Y. Geng, J. Chen, R. Fu, G. Bao, and K. Pahlavan, "Enlighten wearable physiological monitoring systems: On-body RF characteristics based human motion classification using a support vector machine," *IEEE Trans. Mobile Comput.*, vol. 15, no. 3, pp. 656–671, Mar. 2016.
- [8] M. Meina, A. Janusz, K. Rykaczewski, D. Slezak, B. Celmer, and A. Krasuski, "Tagging firefighter activities at the emergency scene: Summary of AAIA'15 data mining competition at knowledge pit," in *Proc. Fed. Conf. on Comput. Sci. and Inf. Syst.*, Lodz, Poland, Sep. 2015, pp. 367–373.
- [9] J. Rantakokko, P. Strömbäck, and P. Andersson, "Foot- and knee-mounted INS for firefighter localization," in *Proc. ION Int. Technical Meeting*, San Diego, CA, Jan. 2014.
- [10] J. Nedder, *Fire Service Rapid Intervention Crews: Principles and Practice*. Jones & Bartlett Learning, Apr. 2014.
- [11] J. O. Nilsson, A. K. Gupta, and P. Händel, "Foot-mounted inertial navigation made easy," in *Proc. IEEE Int. Conf. on Indoor Positioning and Indoor Navigation*, Busan, South Korea, Oct. 2014, pp. 24–29.
- [12] F. Wang and Z. Zhao, "A survey of iterative closest point algorithm," in *Chinese Autom. Congress*, Jinan, China, Oct. 2017, pp. 4395–4399.
- [13] J. Nilsson and P. Händel, "Recursive Bayesian initialization of localization based on ranging and dead reckoning," in *Proc. IEEE/RSJ Int. Conf. Intell. Robots and Syst.*, Tokyo, Japan, Nov. 2013, pp. 1399–1404.